



PROCUREMENT EXECUTIVE, MINISTRY OF DEFENCE

AERONAUTICAL RESEARCH COUNCIL

CURRENT PAPERS

On Three-Dimensional Flow in Centrifugal Impellers

by J. Moore, J. G. Moore and M. W. Johnson

University Engineering Department, Cambridge

RECEIVED
PROCUREMENT
DEPARTMENT
CAMBRIDGE

LONDON: HER MAJESTY'S STATIONERY OFFICE

1977

£2.50 net

ON **THREE-DIMENSIONAL** FLOW IN CENTRIFUGAL **IMPELLERS**

- by -

J. Moore, J.G. Moore and **M.W.** Johnson

SUMMARY

Evidence of non-uniform flow at the exit of centrifugal impeller **passages** is discussed and a **Rossby** number $W/\omega R_n$ which governs the stable location of wake flow in the exit plane of an impeller **is** presented. In impellers with large **Rossby** numbers the stable location of the wake **is** on the shroud wall; wakes on the suction side wall are stable in **impellers** with low **Rossby** numbers.

The ability of a marching-integration procedure to compute a three-dimensional rotating flow with large secondary velocities leading to the formation of a wake is demonstrated. A possible approach to the calculation of three-dimensional impeller flow **is** suggested.

	<u>content</u> 8
page	
3	Introduction
3	Non-uniform flow at impeller exit
5	Secondary flow
9	Observations of three-dimensional flow In impellers
13	Influence of impeller exit flow on diffuser performance
14	Wake flow or back-flow ?
15	Requirements for a calculation procedure
17	A marching integration calculation procedure for impeller flowe
18	Linearization of the momentum equation
19	Uncoupling the s₁ momentum equation
20	The secondary flow momentum equations
21	The finite difference grid
22	Calculation of flow In a rotating radial-flow passage
23	Symmetrical inlet flow
25	Asymmetric inlet flow
29	Concluding remarks
30	Acknowledgement
31	References
34	Figures

Introduction

The flow **in** a centrifugal pump or compressor **is** a complex **viscous** three-dimensional flow **in** which the effects of rotation and curvature promote the development of non-uniform flow. Thus, while the Inlet flow may have uniform properties and the outlet flow may also be approximately uniform, the work Input and the efficiency of the machine **are** governed by the non-uniform flow which is delivered by the Impeller to the **diffuser**.

It is therefore necessary to **have** a detailed understanding of the development of the three-dimensional flow in the rotating Impeller and its subsequent development **in** the stationary diffuser, if one is to calculate and predict the performance of centrifugal machines.

Non-uniform flow at impeller exit

Non-uniform velocity profiles **at** the **exit** of centrifugal impeller passages have been observed for over 50 years. In fact, even before Prandtl's famous paper on the boundary layer, there was a suggestion in 1902 by **J.A.** Smith (1) (reported by Gibson (2)) that under certain conditions the flow tends to leave the leading face (suction **side**) of a centrifugal pump Impeller passage. The flow then passes along the trailing face (**pressure** side) and there is a region

of "dead" fluid on the leading face. This work and the classic work of Carrard (3,4) In 1923 was concerned with flow in two-dimensional radial-flow impellers. Carrard modelled the impeller flow as "le Jet et la zone neutre" in what appears to be the first use of the "jet-wake" flow model. However, the concept of a neutral zone or wake was not new in 1923 and Carrard states that "the hypothesis of the existence of a neutral zone is not new in Itself: it has long been supposed that the channels of (centrifugal) wheels must not work with a uniformly filled cross-section."

Carrard made pressure measurements in centrifugal impellers which showed wake flows associated with separation at the leading edge of the Impeller blades on both the suction side at low flow rates and the pressure side at high flow rates. But he also showed that at certain intermediate flow rates the neutral zone started along the suction surface away from the Impeller inlet. He calculated the velocity distribution in the jet using Flugel's (5,6) streamline curvature method and he assumed a zero velocity for the fluid in the wake. Thus, he was able to obtain remarkably good agreement between the measured and calculated velocity distributions and pressure-rise characteristics of his impellers over their whole flow range.

This two-dimensional picture of a jet-wake flow was used to explain observed impeller flow for many

years (7-10). Indeed, in the slow speed rig used by **Cheshire** (11) to study impeller flow during the development of the early jet engines, it was found that there was "an intense region of high radial velocity at the driving face, the velocity diminishing rapidly towards the trailing **face,* the total** head loss increasing rapidly **in this direction** also." Cheshire concluded that "this state can only be caused by total head loss at the trailing face before entering the radial portion, and **this** is of such magnitude as to represent a complete breakaway of the flow," and his analysis of flow incidence angles at the impeller inlet supported **this** conclusion.

Secondary Flow

Evidence of a jet-wake flow that was not uniform from hub to shroud was presented by Kearton (8) in 1933. But the study of the three-dimensional character of impeller flows did not begin until the 1950's when several papers (12-15) were published on the generation of a **streamwise** component of vorticity in flows in curved and rotating passages. These studies considered the **inviscid** development of flow containing vorticity initially oriented perpendicular to the flow direction. They gave a quantitative understanding of the development of secondary flow in regions where viscosity

***N.B.** Cheshire (11) refers to the trailing face (suction side) of the impeller blade while Gibson (2) refers to the trailing face (**pressure** side) of the impeller passage.

were unimportant and a qualitative picture of **secondary** flow elsewhere. Thus, based on the **results** of his study of **incompressible** flow **A.G. Smith** (15) presented a **qualitative** discussion of the secondary **flows** in the Impeller of a centrifugal **compressor**.

The equations governing the development of the **streamwise** vorticity along a relative streamline which was derived by Smith (15) has recently been presented in the following simple form by Hawthorne (16);

$$\frac{\partial}{\partial s} \left(\frac{\Omega_s}{W} \right) = \frac{2}{\rho W^2} \left(\frac{1}{R_n} \frac{\partial p^*}{\partial b} + \frac{\omega}{W} \frac{\partial p^*}{\partial z} \right) \quad (1)$$

Here $p^* = p + \frac{1}{2} \rho (W^2 + \omega^2 r^2)$ is the rotary stagnation pressure, W is the fluid velocity relative to the rotor and ωr is the rotor tangential velocity; and the equation is expressed in streamline coordinates where s is the streamline direction, n the normal direction and b the binormal direction. The two terms contributing to the generation of the **streamwise** vorticity Ω_s are due to curvature of the streamlines with radius R_n and to rotation with angular velocity ω about the axle of rotation z . They are associated with gradients of rotary stagnation pressure in the binormal and axial directions, respectively.

Smith (15) considered the generation of streamwise vorticity in the axial inducer of the Impeller where the relative tangential velocity of the inlet flow is

reduced and in the **radial** section near the impeller outlet. In the inducer he noted that boundary layers on the hub and shroud walls of the inlet duct would produce radial gradients of p^* which would combine with the tangentially oriented radius of curvature to produce streamwise vorticity. This vorticity would convect fluid with low p^* towards the suction side of the passage along both the hub and shroud walls. In the radial section of the Impeller boundary **layers** on the hub and shroud walls produce gradients of p^* in the axial direction which would combine with the rotation to produce more **streamwise** vorticity. Again this vorticity would convect **fluid** with low p^* towards the suction side.

Smith noted that Cheshire (11) had found a region of fluid with low p^* on the suction side of his impeller passage and he made two **interesting** observations on this fact. Firstly, he observed that if all the fluid with low p^* were located on the suction side in the radial part of the impeller then there could be no further generation of streamwise vorticity. In fact, the condition that p^* becomes smaller **as** the suction side of the radial channel is approached **is** a stable one. Secondly, the two processes for generating streamwise vorticity which he described will result in a tendency for the frictional boundary layer generated

on the channel walls to be swept to the suction **side** of the channel.

Actually, there **is** a third and possibly more important **process** for generating **streamwise** vorticity and **this is** associated with the curvature from the axial to the radial **directions** and with tangential gradients of p^* . Thus, **this** third process **will** influence boundary layer fluid on the suction and pressure **sides** of the impeller **passage** and It **will** generate **streamwise** vorticity such that **this** fluid **will** tend to migrate **towards** the shroud wall. In two dimensional Impellers this effect **will** be **negligible** and fluid with low p^* **will** tend to **settle** uniformly over the suction wall **as** observed by Carrard (3). In three dimensional Impellers, however, It can be a large effect and the fluid with low p^* is often found either **in** the **shroud-** suction-side corner or **completely** on the shroud wall.

Observations of Three-Dimensional Flow in Impellers

Substantial evidence for the **existence** of three dimensional flow in centrifugal impellers has been obtained since 1950, and the flows observed are in general agreement **with** the secondary flow picture outlined above.

A major **programme** of research to investigate the flow in the impellers of centrifugal compressors was conducted by NACA and the results of these investigations were **summarised** by Hamrick (17) in 1955. Hamrick presents the **results** of detailed measurements (18) of static **pressure**, stagnation pressure and velocity in an essentially **two-dimensional** radial-flow impeller. **This** was tested over a range of flow rates at a constant speed and the results show the effects of off-design flow **angles** at the impeller inlet, secondary flows and flow **through** the tip clearance between the blades and the stationary shroud wall.

At approximately one-half the design flow rate there was separation at the inlet **on** the suction side of the blades near the shroud. The fluid with low p^* associated with this separated flow passed down the **channel** and flowed from the shroud-suction-side corner until it was distributed approximately uniformly over the suction side wall - the **stable** location in the

two-dimensional Impeller. Towards the **exit** of the impeller the hub-nhroud height of the impeller passages became small compared with the blade-to-blade wldth of the **passage (1:5.5)**. Then the flow through the tip-clearance (-3.3 %) had a **significant effect** on the flow in the Impeller passages; It **caused** secondary flows which tended to extend the region of low p^* fluid onto the shroud wall.

At approximately 1.5 times the **design** flow rate there was separation at the Inlet on the pressure **side** of the blades again near the shroud. The fluid with low p^* was convected by secondary flow **across** the **shroud** wall to a position near the suction side where It remained, showing no tendency to move onto the **suction** slde wall. **This** suggests that the Influence of the curvature from the axial to the radial direction on the generation of **streamwise vorticity** is relatively larger than the influence of rotatlion. The relative importance of curvature and rotation **as** influences on secondary flow may be **estimated using** the **Rossby** number $\frac{W}{\omega R_n}^*$

* Hawthorne (16) and **Lakshminarayana** and Horlock (19) consider the relative Importance of rotatfon and curvature in the plane of rotation, such as may be found with forward or backward curved Impeller blades. They **use** a **Rossby** number **with** the corresponding radius of curvature and they comment that in centrifugal compressors their **Rossby** number "**is** unlikely to be greater than **1/4**, so that rotation induced **secondary vorticity** dominates."

(see equation (1)). Since the **rotation** rate ω and the radius of curvature R_n of the flow from the **axial** to radial **directions** were fixed for the constant speed tests on the NACA impeller, the influence of curvature **will** become more important at **high flow rates**. For the test results presented by Hamrlck, the **values** of the Roeby number may be estimated to be $1/4$ at the **design** flow rate, $3/8$ at 1.5 times **design** flow and $1/8$ at 0.5 times design flow. These **figures suggest** that rotation was important at all flow rates, that rotation was dominant at low flow rates and that curvature and rotation were of approximately equal importance at the **high flow rates** in the NACA tests.

At the design flow rate the **loss** of stagnation pressure at the inlet **was** relatively small **as** the flow did not separate from the blade **surfaces**. Thus the secondary **flows** were associated with boundary layer growth. However, as the outlet **cross-sectional** area of the impeller passage **was** approximately equal to the inlet throat **area**, the **changes in** relative velocity were small and the boundary layers did not thicken appreciably. Fluid with low p^* accumulated on the suction side wall due to the action **of secondary flows**, but the stagnation pressure losses associated with **this** fluid were small compared with the **losses** caused near the shroud wall by flow through the **tip-clearance**.

It may be concluded from Hamrick's results that the flow distribution at the exit of a centrifugal impeller can be strongly influenced by secondary flow. The secondary flow is caused by the curvature and rotation of the impeller passage. The final location of low stagnation pressure fluid in the cross-sectional plane at the exit of the Impeller depends on the relative magnitude of the two effects and on how far the generation of streamwise vorticity has progressed. Even in the nearly two-dimensional Impeller used by Hamrick the effects of curvature were significant at high flow rates and the fluid with low stagnation pressure moved towards the shroud wall.

An impeller in which the effects of curvature are even more important has been tested recently by Eckardt (20). At the test condition of 14000 RPM and a mass flow rate of 5.31 kg/s the value of the Rossby number $W/\omega R_n$ for Eckardt's impeller is approximately 1.0. An extrapolation of Hamrick's results suggests that fluid with low stagnation pressure will accumulate at the shroud wall and this is exactly what Eckardt observed. Eckardt comments in answer to discussion of his paper that "the circumferential position of its (the wake's) core, in the presented case at $y/t = 0.65$, shifts between $y/t = 0.5 - 0.8$, depending on mass flow and speed." Although he offers no further comment, it is clear from the present argument that a stable wake location closer to the suction side ($y/t = 0.8$) is

expected at **high** speed and low flow, and a stable wake location towards the middle of the shroud wall **is expected** at low speed and high flow.

Influence of Impeller **Exit Flow** on Diffuser Performance

A question which **naturally arises** at this point **is** where in the impeller exit plane would the designer wish to have the low stagnation pressure fluid if he had the choice? Indeed, how **is** the performance of the diffuser influenced by the location?

Much attention has been concentrated on the subsequent development of jet-wake flow in **vaneless** diffusers. Several workers (21-23) have considered the case of jet and wake flows **which** are uniform between the hub and shroud walls. But **as** we have seen such flow is associated with a small **Rossby** number, and even the nearly two-dimensional **impeller** of **Hamrick (18)** only produced axially uniform flow at low flow rates. Thus, It **is** a **special** case and the work of **Ellis (24)** and **Rebernik(25)** has shown **that** this **is** only one of many different exit flow **distributions** and it leads to only one of many flows **in** the **vaneless** diffuser. Furthermore, as the **Rossby** number changes **with** flow rate, the Impeller exit flow **distribution will** also change unless the **Rossby** number **is** very large or very small. The designer needs to know what flow to produce at the impeller exit and how to produce it.

Wake Flow or Back-Flow ?

The accumulated low stagnation pressure **fluid** **observed** by Hamrick and Eckardt had a **significant** radial velocity even at the **exit** of the impeller. In the case of Hamrick's impeller this was due to **the relatively** constant area of the passages and even when the blade unloaded on the suction **side** the fluid had sufficient momentum to **continue** down the channel. In Eckardt's impeller the low momentum fluid **was** away from the suction side and so it **did** not experience the **unloading** of the blades. In **both** cases this fluid **is** a significant fraction of the total mass-flow rate and Eckardt **states** that it **is** about **15 %** of his Impeller flow. In **both** cases also this wake flow exhibits no **reverse** flow. It **is** not a separated flow in the sense of two-dimensional boundary layer separation; It **is** instead an accumulation of low momentum fluid which has flowed towards the low pressure regions of the channel by the action of secondary flows. These observations are **of** great importance to the designer for they indicate that he may be able to calculate the wake flow as well as the jet flow by marching-integration methods, starting at the impeller inlet and marching to the exit.

Requirements for a Calculation Procedure

It is apparent from the **discussion** above that the calculation of the performance of centrifugal machines will be complex in all but the simplest cases. Carrard was able to calculate the pressure rise in his two-dimensional Impellers **using** a simple two-dimensional Jet-wake model and considering only the flow in the rotor. But two-dimensional flow **is a special case** and practical machines with an axial inlet and a radial outlet exhibit three-dimensional flow with secondary flow velocities that can be locally large compared with the **through** flow velocity. An extension of Carrard's **ideas** is required and this must include a calculation of the three-dimensional flow including the jet and the wake flow and allowing the location of the wake to be governed by secondary flow. It must **also** include an analysis of the **subsequent** development of the non-uniform impeller exit flow as it passes **through** a **vaneless** diffuser and then possibly through a **vaned diffuser** as well.

The sources of fluid with low stagnation pressure which accumulate **as** a wake flow are

- 1/ boundary layers on the walls of the impeller channels,
- 2/ separated flow at the impeller inlet,
- 3/ boundary layer flow and regions of low stagnation pressure in the inlet flow,

4/ flow through the tip-clearance between the impeller blades and the stationary shroud wall.

A calculation procedure for impeller flow should include each of these sources and a method of calculating their convection towards the wake. The convection **is** influenced by curvature in the inducer and **in** the axial to the radial bend and by rotation. It **is** clear that only a general **calculation** scheme for three-dimensional flow will handle all **these** effects simultaneously.

Moore (26) has shown that such calculations can be made for a relatively simple flow in the rotating radial-flow passage shown in Figure 1. In Moore's flow the sources of low **stagnation** pressure fluid were the boundary layers and the inlet flow. But **his** simple analysis included only the effects of the boundary layers and neglected secondary flow in the potential flow which was assumed to have uniform stagnation pressure. **Nevertheless**, he was able to calculate the development of the boundary layers on all four walls of the rectangular passage and he showed that secondary flows developing on the hub and shroud walls were of **sufficient** magnitude to convect low-momentum boundary layer fluid to a wake on the suction side of the **passage**. Moore's calculation procedure was **specifically intended** for his simple geometry. The potential flow analysis

applied to simple two-dimensional radial flow and the boundary layer analysis was **specific** to the walls of **his** rectangular passage. The procedure can not be easily extended to more complex **geometries**. However, It contains a **calculation** of the whole flow and it allows the migration of boundary layer fluid towards a wake. A method with more generality which **includes** these features **is** necessary for Impeller flow calculations.

A Marching-Integration Calculation Procedure for Impeller Flows

A **marching integration** procedure for the **calculation** of three-dimensional **parabolic flows** has been **suggested** by Patankar and Spalding (27). **This** may be extended and combined **with** the **results** of an **inviscid streamline-curvature** calculation to **give** an economical procedure for calculating three-dimensional **viscous** flow **throughout** an Impeller passage.

The procedure **hinges** on the **simultaneous** solution of the continuity and momentum **equations** in **finite** difference form. These equations for steady flow may be written in vector form as

$$\nabla \cdot (\rho \underline{V}) = 0$$

and

$$(\underline{V} \cdot \nabla) \underline{V} = \underline{X} - \frac{1}{\rho} \nabla \cdot \underline{\pi} ,$$

where **X** is the body force vector and **π** is the stress tensor (28).

For a marching Integration to be possible we must choose the **direction** of **marching** such that the velocity **always** has a positive component **in this** direction. Since **impeller** geometries vary widely we consider the flow in general orthogonal coordinates s_1, s_2, s_3 , with scaling **factors** h_1, h_2, h_3 and velocity components u_1, u_2 and u_3 . The marching Integration proceeds in the s_1 direction, which closely follows the direction of bulk flow.

Linearization of the momentum equation.

To Integrate the momentum equation over a forward step we first divide the equation into two parts; the first part containing unknown quantities and the second containing quantities which may be calculated from upstream values and are thus known. **Also** we linearize the equations with respect to the unknown velocity **components**. We then combine the continuity and momentum equations to **give** momentum equations which can be used to calculate the three unknown velocity components u_n . **These** equations may be written in the following form

$$\frac{1}{h_1 h_2 h_3} \left\{ \frac{\partial}{\partial s_1} (\rho h_2 h_3 u_1 u_n) + \frac{\partial}{\partial s_2} (\rho h_1 h_3 u_2 u_n) + \frac{\partial}{\partial s_3} (\rho h_1 h_2 u_3 u_n) \right\}$$

$$= \frac{1}{h_1 h_2 h_3} \left\{ \frac{\partial}{\partial s_2} \left(\frac{h_3 h_1 \mu}{h_2} \frac{\partial u_n}{\partial s_2} \right) + \frac{\partial}{\partial s_3} \left(\frac{h_1 h_2 \mu}{h_3} \frac{\partial u_n}{\partial s_3} \right) \right\} - \frac{1}{h_n} \frac{\partial p}{\partial s_n} + F_n$$

for $n = 1, 2, 3$

In **these** equations, the left hand **side represents** part of the convection term $(\underline{V} \cdot \nabla) \underline{V}$. The other part of the convection term **is** due to curvature of the coordinate system and together with the body force **it is** included **as** part of the term, F_n , which is considered known. The term involving the **stress** tensor Π is separated into a pressure term, viscous terms which contain the unknown velocity u_n and **additional** viscous terms which are also included in the known F_n . The choice of which **viscous terms** to take as known and which as unknown may seem arbitrary. However the above choice has the advantage that the equations are of the same form. Thus-when they are expressed in **finite** difference form the coefficients of the unknown velocity components are the same **for** all three equations. **Since** the marching **integration** proceeds in the s_1 direction the **viscous** terms due to velocity gradients in this direction are neglected.

Uncoupling the s_1 momentum equation

The linearized momentum equations are coupled together by the **pressure** p so that the velocity components also **satisfy** continuity. The momentum equation for u_1 depends only indirectly on the transverse pressure **gradients** $\partial p / \partial s_2$, $\partial p / \partial s_3$ and **is** therefore not sensitive to small errors **in** these gradients.

These transverse **pressure** gradients can be **estimated** using **inviscid** streamline curvature **calculations**.

Therefore, In the calculation procedure the **pressure** \bar{p} In the u_1 momentum equation is distinguished from the pressure p in the momentum equations for the secondary flow **velocities** u_2 and u_3 ; and It is assumed that the transverse **gradients** of \bar{p} are known **throughout** the flow from streamline curvature calculations made prior to the **marching** integration. The pressure \bar{p} is corrected uniformly at each step so that, over the cross-section of the passage, the correct mass flow is obtained.

The secondary flow momentum equation

The momentum equations for the secondary flow velocities u_2 and u_3 may be solved in finite difference form once a pressure distribution is chosen. The problem is to **choose** the pressure distribution so that the velocity components also satisfy continuity.

In the procedure, an estimated pressure distribution p^e is used to obtain estimates of u_2 and u_3 . We then assume that corrections p^c in the pressure are related to corrections, u_2^c and u_3^c , of the velocity components by the abbreviated momentum equation,

$$\frac{\rho u_1}{h_1} \frac{\partial u_n^c}{\partial s_1} \approx - \frac{1}{h_n} \frac{\partial p^c}{\partial s_n}$$

This expression is substituted into the continuity equation and the resulting equation for the pressure correction p^c is solved. The improved pressure estimate $p^o + p^c$ is now used in the momentum equations to obtain improved values of u_2 and u_3 . This correction method can be improved but it was found satisfactory for the present calculations.

The finite difference grid

The number of grid points required are kept to a minimum by using a non-uniform grid spacing with linear profiles of the flow properties between the grid points. This allows grid points to be concentrated in the near-wall regions where they are required for the accurate calculation of the secondary flows which convect fluid with low p^* .

The finite difference equations for continuity and momentum conservation are formed by integrating over control volumes with boundaries midway between the grid points. These equations are solved using the tri-diagonal matrix-algorithm double-sweep method of solution. This and other aspects of the procedure are similar to the Patankar and Spalding method,

Equation 9 for the conservation of energy and other properties can be written in a form similar to the momentum equation and thus can be included in the marching integration procedure.

Calculation of Flow in a Rotating Radial-Flow Passage

The applicability of this procedure to the calculation of impeller flow **will be demonstrated** by calculating the medium-flow measured by Moore (26).

Moore measured the flow development in the rotating radial-flow **passage** shown in Figure 1. The figure shows a schematic and a **sectional** view of the test-section which was mounted on a rotating turntable. The test-section had a constant height of **3** In. and the **side walls** were **radii** with an included angle of **15°**. The length of the test-section was **24 in.** and the square inlet was at a **radius** of 12 In. The rotational speed was 206 RPM.

At the medium flow rate the mean velocity at the inlet to the test section was **54.9 ft/s**. At **this** flow rate, Moore measured the three-dimensional flow **distribution**, **0.5** In. downstream of the inlet, and the results of the measurements are **shown** in **Figure 2**. In the present calculations two flow distributions have been **used** to start the marching integration. One based on the measured **asymmetric three-dimensional** velocity distribution at **x = 0.5 inches**, and, for **comparison**, a second distribution assuming a purely radial inlet flow **symmetrical** about the mid-height of the passage.

Moore's flow was incompressible and we have adopted a **simple** viscosity model **which uses** the **Prandtl mixing** length to calculate the turbulent contribution

to the **viscosity**. The mixing length was taken as the **smaller** of 0.08δ and $0.41y$, where δ is the boundary layer thickness and y is the **distance** to the nearest wall. Negative values of **radial velocity** were not allowed and all the velocity components were set to zero at the **walls**. The transverse pressure gradient through the flow were taken as $\frac{\partial \bar{p}}{\partial s_2} = 2\rho\omega\bar{u}_1$ $W = 66 \text{ kN/m}^2$ and $\frac{\partial \bar{p}}{\partial s_3} = 0$, where $s_2 = -Y/W$ and $s_3 = Z/h$ and the symbols are defined in Figure 1. This value of $\frac{\partial \bar{p}}{\partial s_2}$ is consistent with Moore's measurements which indicated a constant static **pressure** difference between the pressure and **suction** side walls.

Symmetrical inlet flow

The velocity distribution at the inlet was **chosen** to be symmetrical about the **mid-height** of the rotating **passage** and it was assumed that at the Initial **station** the flow was radial. The marching **integration** was performed for one half of the channel using a **13 by 8 grid** and a symmetry condition was applied at the **mid-height** plane. The Inlet flow was assumed to consist of a potential flow core with **uniform** stagnation pressure and boundary layers of uniform thickness on each of the three walls. **Initially 5 points** represented each boundary layer **profile**, grid points being located at 0, 1, 5, 20 and 100 per cent of the Inlet boundary layer thickness. The results of the flow calculations are presented In **Figures 3-7**.

Figures **3** and **4** show contours of radial velocity,

as a fraction of the local mean **velocity**, over **six** cross-sectional **planes** in the channel. A pictorial representation of the corresponding secondary **velocities** **is** shown in Figures 5 and 6, and the development of the radial velocity at the mid-height plane of the channel is shown **with** the measured development in Figure 7.

Secondary flows transport low momentum fluid from the pressure side boundary layer into the **suction side** layer and these, together with the corresponding **movement** of the potential flow towards the **pressure** side, are shown in Figures 5 and 6. In these calculations the tangential velocity remained approximately constant across the top and bottom walls and the **initial** large cross flows from the pressure side **corners** result from the deceleration **of the fluid** in these corners due to the radial adverse pressure gradient. Between $x = 14.5$ inches and $x = 18.5$ inches fluid with radial velocity less than one half of the mean velocity **flows** from the **pressure side** wall. This fluid and most of the fluid with low p^* accumulates on the suction side and shows an initial tendency to move towards the mid-height of the **passage** as shown in Figures 3 and 4. **Streamwise vorticity** is then generated as seen in the secondary velocities at $x = 20.5$ inches in Figure 6 and **this** vorticity tends to return the fluid with low p^* to its stable location near the suction side wall in this flow which has a Rossby number $W/\omega R_n = 0$.

Fluid with low p^* is continually generated along the pressure side wall and after $x \approx 18.5$ inches in the calculations it is convected first towards the mid-height, then towards the suction side and finally it passes close to the pressure wall as it moves onto the top or bottom wall. This calculated pressure side flow is similar to Taylor-Goertler vortex flow with two complete cells near the mid-height and two 'open' cells in the corners. It shows the complexity which can be caused by small scale effects in impeller flow calculations. This thickening of the pressure side boundary layer in the calculation with the symmetrical inlet flow is shown in Figure 7 and it was not observed in the experiments. However, the general agreement between the calculated and measured radial velocities at the mid-height of the channel is good. The wake develops on the suction side with similar shape and size to the measured wake and it thickens markedly after $x \approx 10.5$ inches as observed.

Asymmetric inlet flow

The measured asymmetric inlet velocity distribution shown in Figure 2 was used with interpolation and extrapolation to obtain the initial secondary velocities shown in Figure 10. The distribution of radial velocity was obtained by using linear interpolation between the nine central measurements, extrapolation of the

potential flow to the boundary layer edges and boundary layers of uniform thickness on each of the four walls. The resulting initial condition is necessarily approximate but it can be used to obtain an estimate of the Influence of non-uniform Inlet flow on the flow development, and ideally It should **result** In better **agreement** with the measurements. The results of these flow calculations using a **13** by **13** grid are presented in Figures 7-11.

Figures 8 and 9 show contours of radial velocity which may be compared **with** the contours obtained for the symmetrical flow shown in **Figures 3** and 4. **Similarly**, the calculated secondary velocities shown In Figures 10 and 11 may be compared with the velocities shown in Figures 5 and 6, and the radial velocity at the **mid-height** plane **is** shown in Figure 7.

The influence of the asymmetric inlet flow dominates the flow initially. **Figure** 10 shows strong secondary flow Into the top corner on the pressure side, **across** the top wall and onto the suction side. The low momentum fluid builds up In two pockets in the corners at the top of the channel and these are evident at **x = 10.5** inches in Figure 8. Figure 9 then shows the migration of the fluid from the pressure side pocket across the top wall to join the bulk of the low momentum fluid near the centreline in the suction-side

wake. Here, **as** In the symmetric flow calculation, wake flow extends along the centrellne **towards** the **pressure** side, especially at $x = 18.5$ Inchea. The secondary **velocities** shown In Figure 11 Indicate that **streamwise** vorticity then develops **which** tends to return **this** fluid to the suction side and **tends** to **distribute** the wake more uniformly over the suction **side** wall.

Figures 8 and 10 also show a comparleon of the calculated velocity dlatribution at $x = 10.5$ Inches with the measured velocity **distribution** at $x = 11$ Inches. The radial and the secondary velocities are In extremely good agreement except near the bottom wall where the calculated boundary layer thlcknesa and the resulting tangential velocities are larger than observed. The relatively low velocities meaasured In the top **pressure-**side corner support the calculated accumulation of a pocket of low momentum fluid, Indeed In taking the measurements Moore noted that at the data point **closest** to the top wall in this corner the **pressure** was "more unsteady".

The **asymmetric** flow calculation gives a thinner pressure-side boundary layer at the channel mid-height than calculated for the symmetric flow. This Is shown In Figure 7, and the difference between the two calculations may be seen quite clearly by comparing

Figures 4 and 9. In the asymmetric flow there is a **relatively** complete transport of boundary layer fluid from the pressure **side** wall by secondary flow. The asymmetric flow calculation also results in an apparently thicker wake on the suction side at $x = 14.5$ Inches and $x = 18.5$ Inches. However, Figure 9 shows that **this is** mostly due to the local accumulation of fluid **with** low p^* on the **centreline** in this calculation, and the **streamwise vorticity** subsequently reorients the wake fluid to give similar wake thicknesses at $x = 20.5$ inches.

Moore's channel was sufficiently long that in both calculations most of the fluid **with** low p^* had accumulated on the suction side wall by $x = 20.5$ Inches. Thus, at this radial location the velocity distributions are very similar in the two calculations. However, the development of the flow in the two cases is quite **different**. The details of the flow development may well have a **significant** effect on the performance of centrifugal machines especially if wake fluid has not reached its stable location at the impeller exit.

Concluding Remarks

It **is** clear that centrifugal machines often have non-uniform flow at the Impeller exit and that **this** flow can have a large effect on performance. Fluid **with** low stagnation **pressure is** found to accumulate in "wake" flows which are often a **significant** fraction of the **mass** flow through the machine. The calculation of the size and location of these wake flows **involves** the calculation of the development of complex **viscous** three-dimensional flow in Impeller geometries. **A** possible approach to the solution of this problem is offered by the combination of a marching-integration procedure for the calculation of parabolic flows with a streamline curvature calculation of the approximate **characteristics** of the primary flow through the machine. The ability of a marching integration procedure to compute a complex three-dimensional flow with large secondary velocities leading to the formation of a wake, has been demonstrated. It appears that an **extension** of this procedure to impeller flow calculations may be facilitated by general. orthogonal **coordinates** which have been used in **this** work.

The **Rossby** number $W/\omega R_n$ which governs the stable location of wake flow at the impeller exit **is** based on the rotation rate ω , the relative velocity W and the radius R_n of the curvature from the axial to the **radial**

direction. Large values of **this** number Indicate that curvature **is** dominant and the stable **location of** the wake **is** on the shroud wall. Small values **signify** the dominance of rotation and a stable wake location on the **suction** side wall. It is Interesting to note that low specific-speed Impellers tend to have low **Rossby** numbers, while high **specific** speed Impellers tend to have **high Rossby** numbers. **Qualitative** understanding of Impeller flow may be obtained by consideration of the generation of **streamwise** vorticity.

Acknowledgement

The computer **calculations** performed **in** this study have been sponsored by **Rolls-Royce (1971)** Ltd. as part of the **Rolls-Royce / Whittle** Laboratory **collaboration** at Cambridge University. The partial support of one of the authors (**J.G.M.**) under this contract **is** gratefully acknowledged. The authors also wish to thank **Mr. 2.H. Timmis** and **Mr. C.M. Pratt** of the Rolls-Royce Helicopter Engine Group for **their** encouragement.

References

1. **Smith, L.A.**, "Notes on Some Exparlmentsl Reserches on Internal Flow in Centrifugal Pumps and Allied Machines", *Engineering*, vol. **Lxxiv** p 763, Dec 5, 1902.
2. **Gibson, A.H.**, *Hydraulics and its Applications*, Constable 1st Ed., 1908.
3. **Carrard, A.**, "Sur le Calcul des Rows Centrifuges", *La Technique Moderne*, T. XV No. 3 pp 65-71 and No. 4 pp 100-104, Feb. 1923.
4. **Carrard, A.**, "On Calculations for Centrlfugal Wheels", translation by **J. Moore**, Univ. of Cambridge, Dept. of **Eng. Report No, CUED/A Turbo/TR 73, 1975.**
5. **Flugel, G.**, "Ein neues Verfahren der graphischen Integration", *Dissertation* Munich, 1914.
5. **Stodola, A.**, *Steam and Gas Turbines Vol. II*, **McGraw-Hill Book Co., Inc, 1927, pp992-997, 1252-1270,** (Reprlnted, **Peter Smith (New York), 1945)**
7. **Fischer, K. and Thoma, D.**, "Investigation of the Flow Conditions in a Centrifugal Pump", *A.S.M.E. Trans., HYD-54-8, 1932.*
8. **Kearton, W.J.**, "Influence of the Number of Impeller Blades on the Pressure Generated In a Centrifugal Compressor and on Its General Performance", *Proc. Inst. Mech. Eng.* Vol. 124, pp 481-568, 1933.
9. **Church, A.H.**, "Centrifugal Pumps and Blowers", 1944, Reprinted, **Robert E. Krieger, Huntington, New York, 1972.**
10. **Dean, R.C., Jr**, "On the Unresolved Fluid Dynamics of the Centrifugal Compressor", *Advanced Centrifugal Compressors, A.S.M.E., Special Publication, pp 1-55, 1971.*
11. **Cheshire, L.J.**, "Centrifugal Compressors for Aircraft Gas Turbines", *Proc. I. Mech E.* Vol. 153, p 440, 1945.
12. **Squire, H.B. and Winter, K.G.**, 'The Secondary Flow in a Cascade of Airfoils In a Non-uniform Stream", *J. Aero. SC.*, Vol 18, pp 271-277, 1951.
13. **Hawthorne, W.R.**, "Secondary Circulation In Fluid Flow" , *Proc. Roy. Soc. A.* Vol. 206, pp 374-387, 1951.

14. Kramer, J.J. and Stanitz, J.D., "A Note on Secondary Flow in Rotating **Radial** Channels", NACA Report 1179, 1954.
15. Smith, A.G., "On the Generation of a **Streamwise** Component of **Vorticity** in a Rotating Passage", Aero. Quart. Vol. 8, pp 369-383, 1957.
16. Hawthorne, W.R., "Secondary Vorticity in **Stratified** Compressible Fluids In Rotating Systems, " Univ. of **Cambridge**, Dept. of Eng. Report No. CUED/A-Turbo/TR 63, 1974.
17. Hamrick, J.T., "Some Aerodynamic Investigations In Centrifugal Impellers", Trans. **ASME**, April 1956, pp 591-602.
18. Hamrick, J.T., Mizisin, J. and Michel, D.J., "Study of Three-Dimensional Flow Distribution Based on Measurements In a **48-Inch** Radial-Inlet Centrifugal Impeller", NACA TN 3101, 1954.
19. Lakshmlnarayana, B. and Horlock, J.H., "**Generalised** Expreselons for Secondary **Vorticity** using Intrinsic **Coordinates**", J. Fluid **Mech.**, Vol. 59, PP 97-115, 1973.
20. Eckardt, D., "**Detailed** Flow Investigations wltln a High-Speed Centrifugal Compressor Impeller", **Trans. ASME, J. Fluids Eng.** Vol. 98, pp 390-402, 1976.
21. Dean, R.C., Jr. and Senoo, Y., "Rotating Wakes In **Vaneless** Diffusers", **Trans. ASME, J. Basic Eng.**, vol. 82, 1960, pp 563-574.
22. Johneton, J.P. and Dean, R.G., Jr., 'Losses in **Vaneless** Diffusers of Centrifugal **Compressors** and Pumps" , **Trans. ASME, J. Eng. Power**, Vol. 88, 1966, pp 49-60.
23. Senoo, Y. and Ishlda, M., "**Behavior** of Severely Asymmetric Flow in a **Vaneless** Diffuser", **Trans. ASME, J. Eng. Power**, Vol. 97, pp375-387, 1975.
24. Ellis, G.O., "A Study of Induced Vorticity in Centrifugal Compressors", **Trans. ASME, J. Eng. Power**, Vol. 06, pp63-76, 1964.
25. Rebernik, B., 'Investigation on Induced Vorticity in **Vaneless** Diffusers of Radial Flow Pumps', Proceedings of the Fourth Conference on **Fluid Machinery**, Budapest, 1972, pp 1129-1139.

26. Moore, J., "A Wake and an Eddy in a Rotating, Radial-Flow Passage (Part 1: Experimental Observations, Part 2: Flow Model)," J. Eng. for Power, Trans. ASME, Ser A, Vol. 95 No. 3, pp 205-219, 1973.
27. Patankar, S.V. and Spalding, D.B., "A Calculation Procedure for Heat, Mass and Momentum Transfer In Three-Dimensional Parabolic Flows", Int. J. Heat and Mass Transfer, 15, pp 1787-1806, 1972.
28. Tsien, H.S., "The Equations of Gas Dynamics", Fundamentals of Gas Dynamics, ed. Emmons, H.W., Oxford Univ. Press, London, 1958.

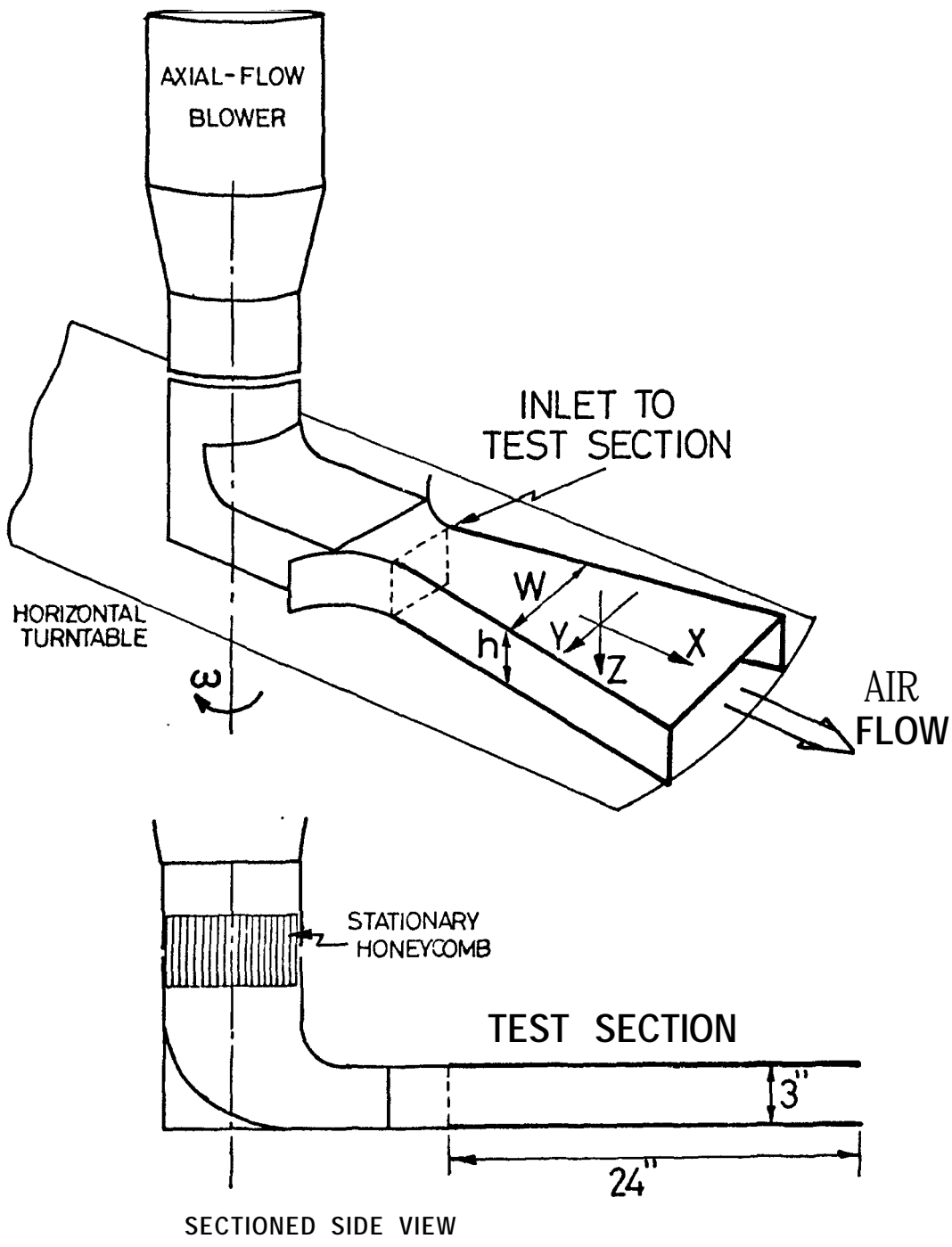


Figure 1. Schematic of Moore's test section.

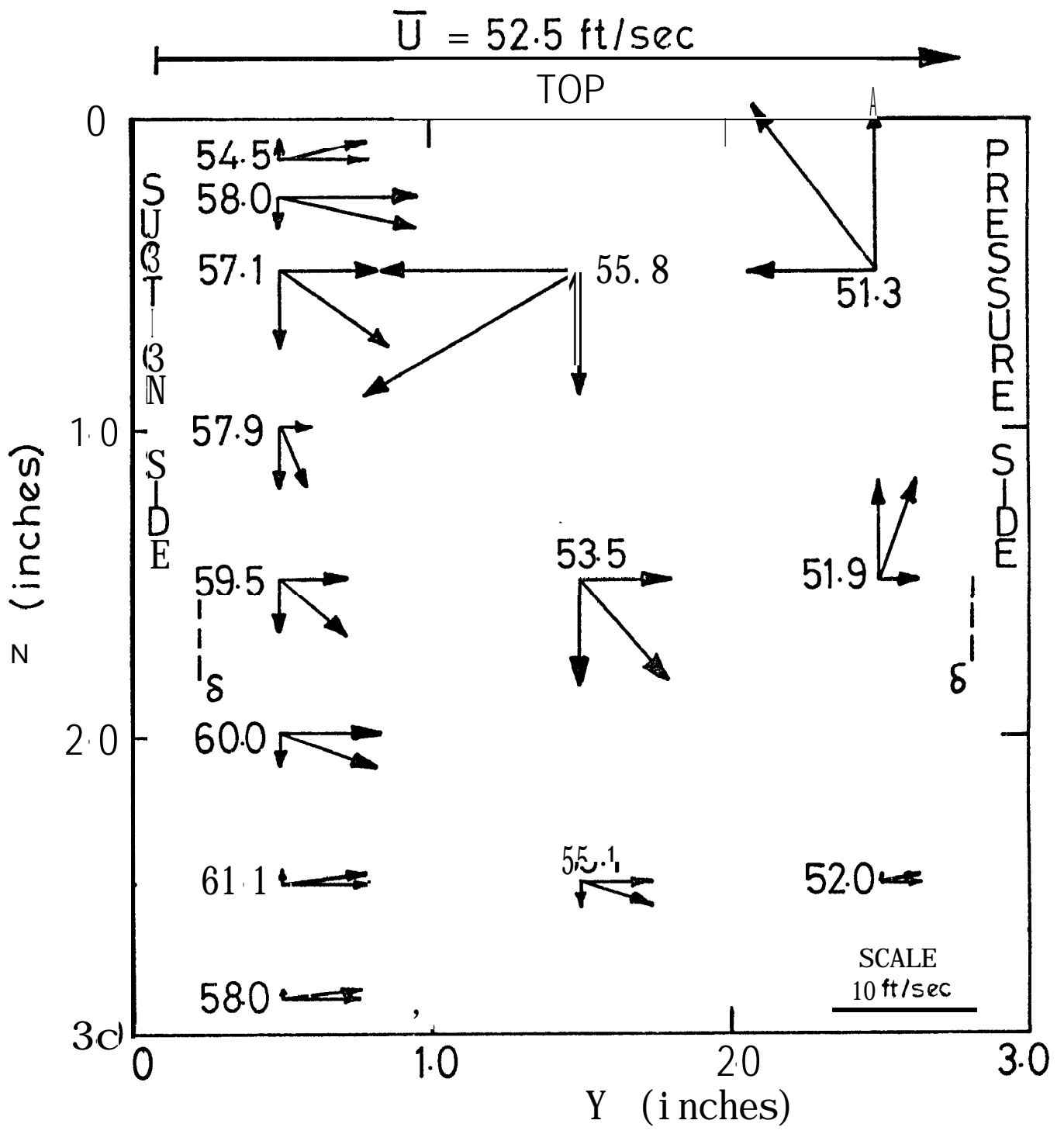


Figure 2. Measured secondary and radial velocities at $x = 0.5$ Inches.

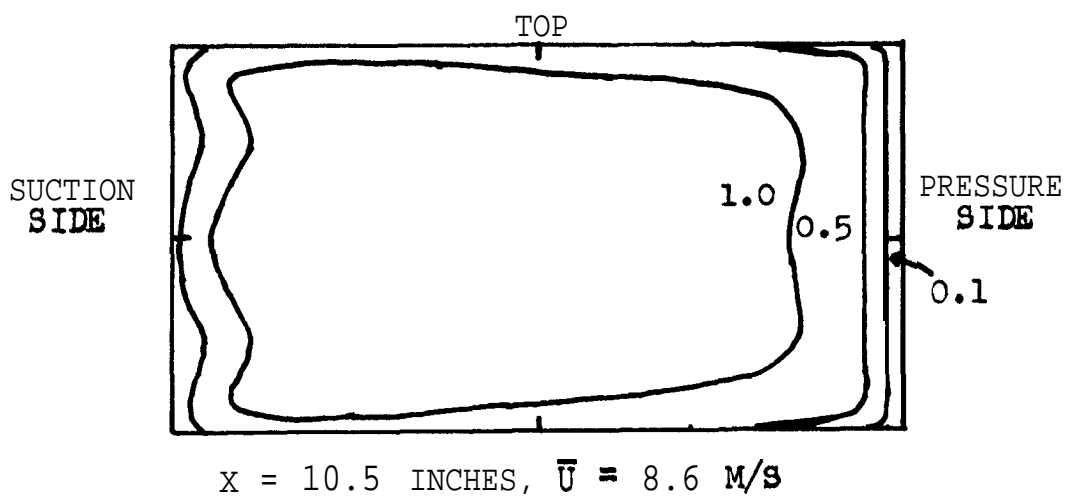
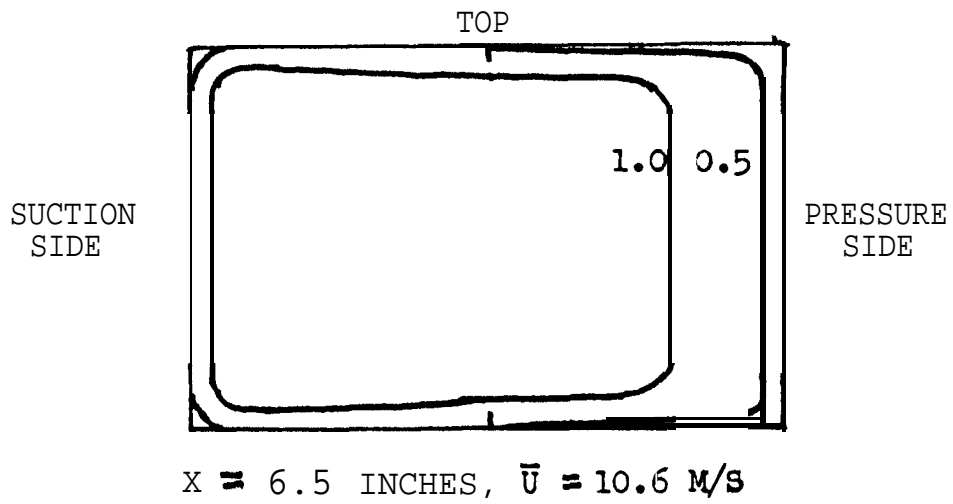
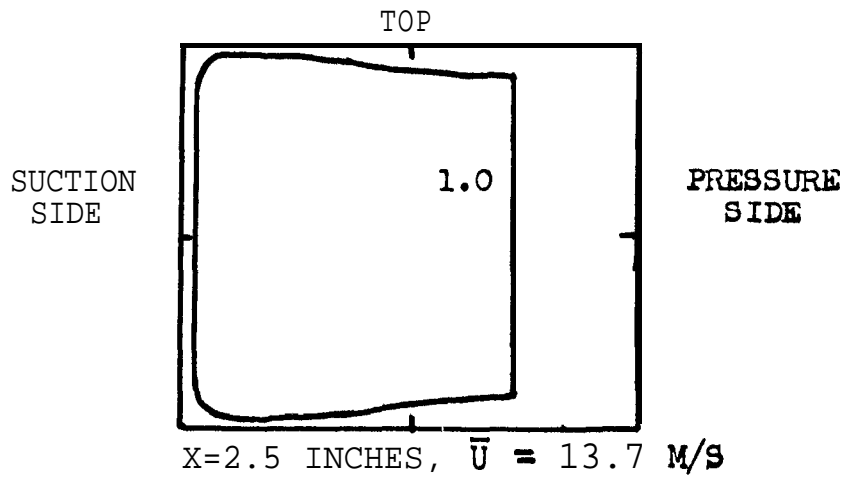


Figure 3. Contours of calculated radial velocity, expressed as a fraction of the local mean velocity, for symmetric flow at $x=2.5$, 6.5 and 10.5 Inches.

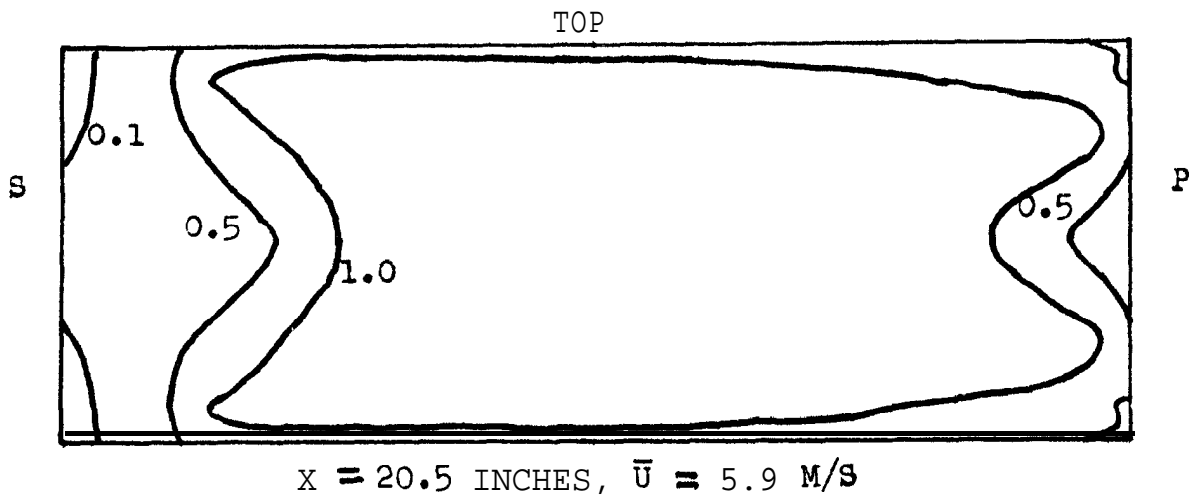
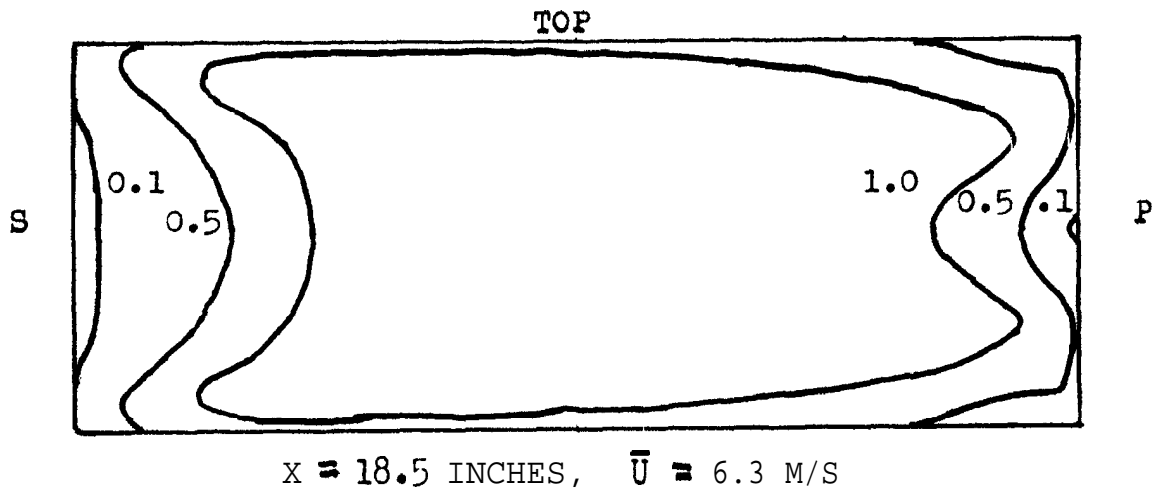
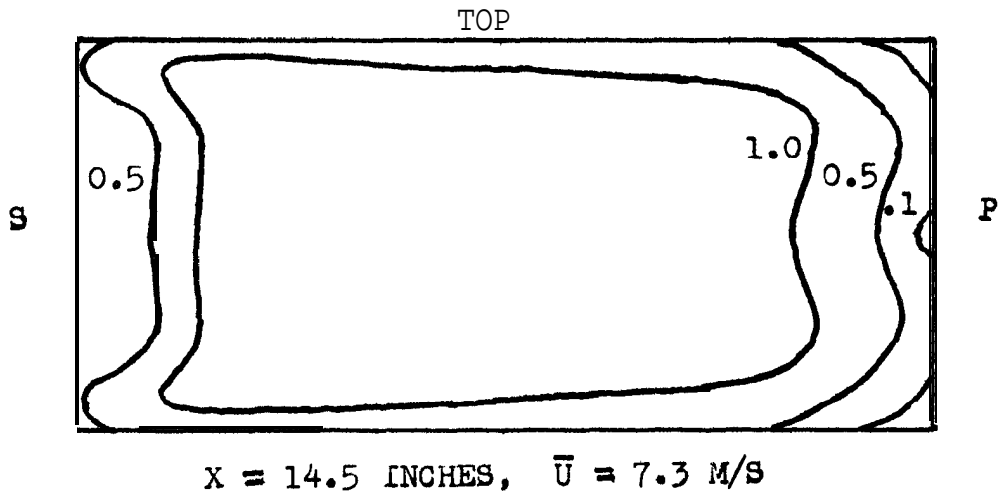


Figure 4. Contours of calculated radial velocity, expressed as a fraction of the local mean velocity, for symmetric flow at x at 14.5, 18.5 and 20.5 Inches.

0 2 4 M/S

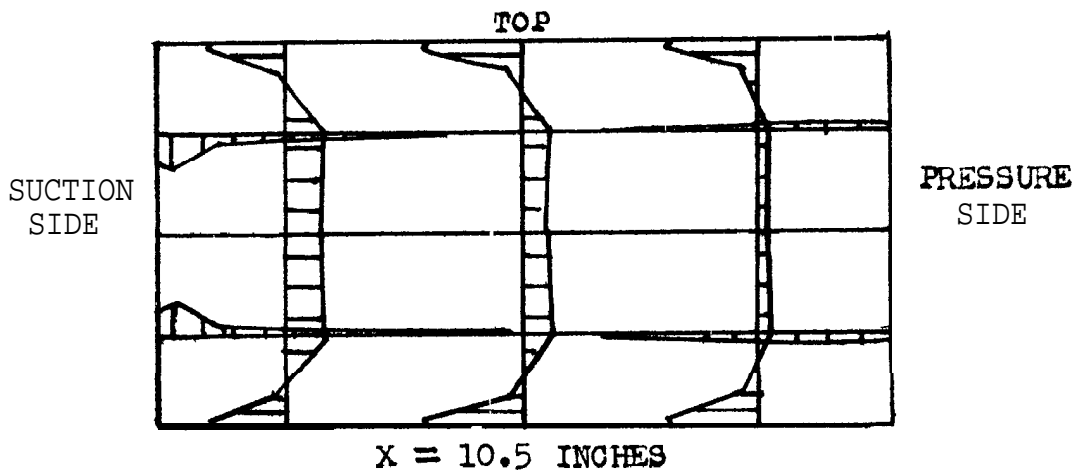
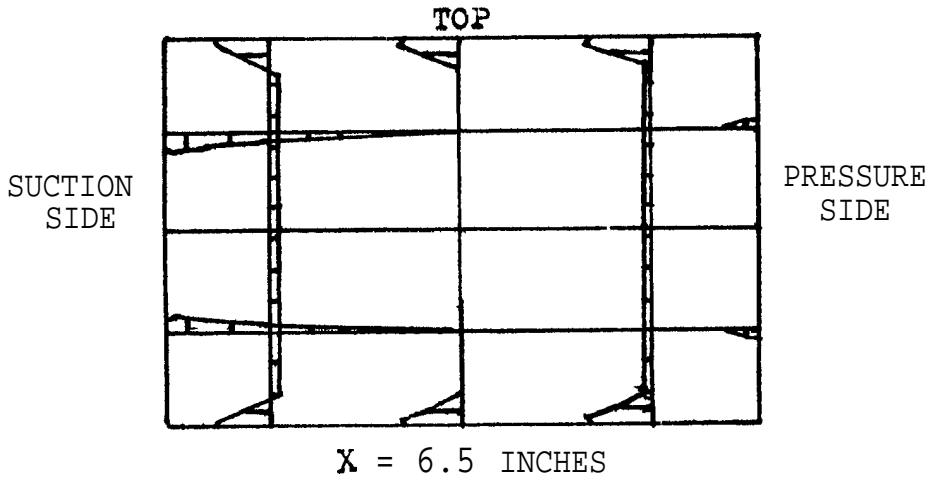
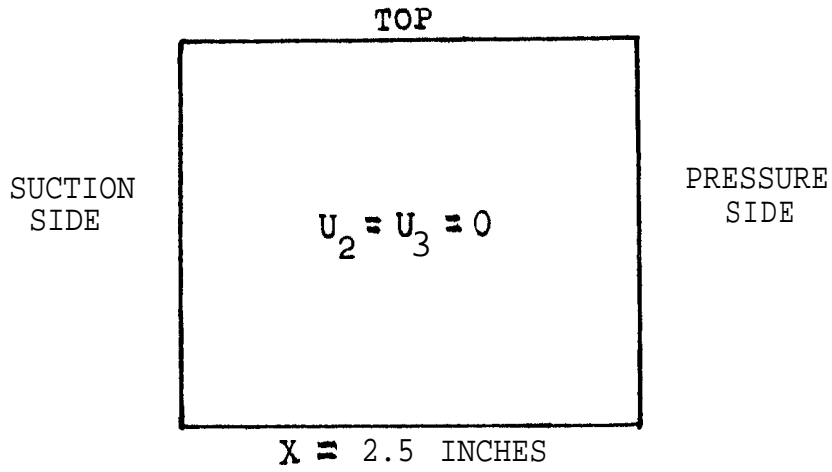
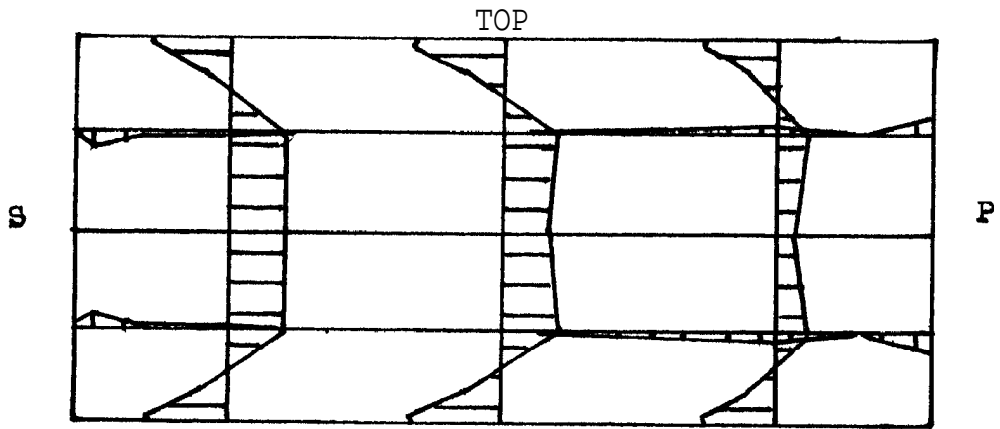
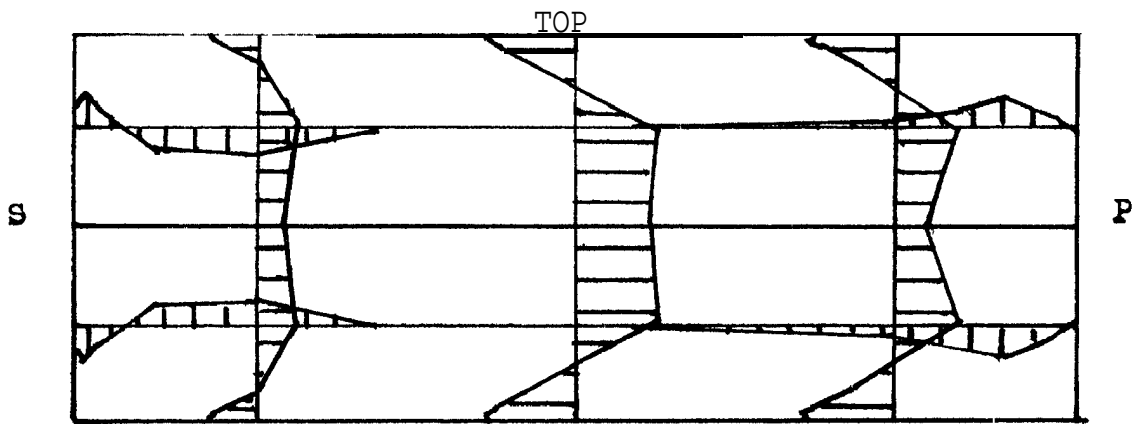


Figure . Calculated secondary velocity distributions for symmetric flow at $x = 2.5, 6.5$ and 10.5 inches.

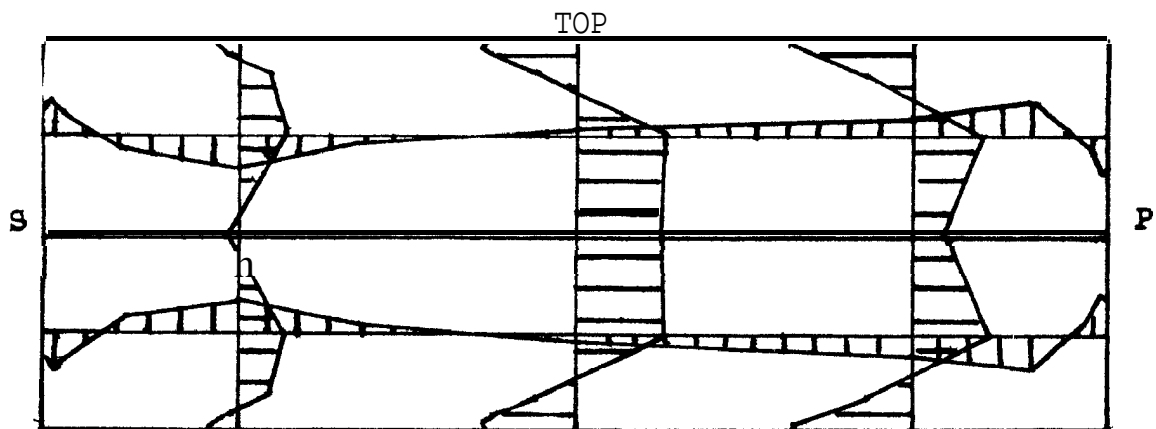
0 2 4 M/S



X = 14.5 INCHES



X = 19.5 INCHES



X = 20.5 INCHES

Figure 6. Calculated secondary velocity distributions for symmetric flow at $x = 14.5, 18.5$ and 20.5 inches.

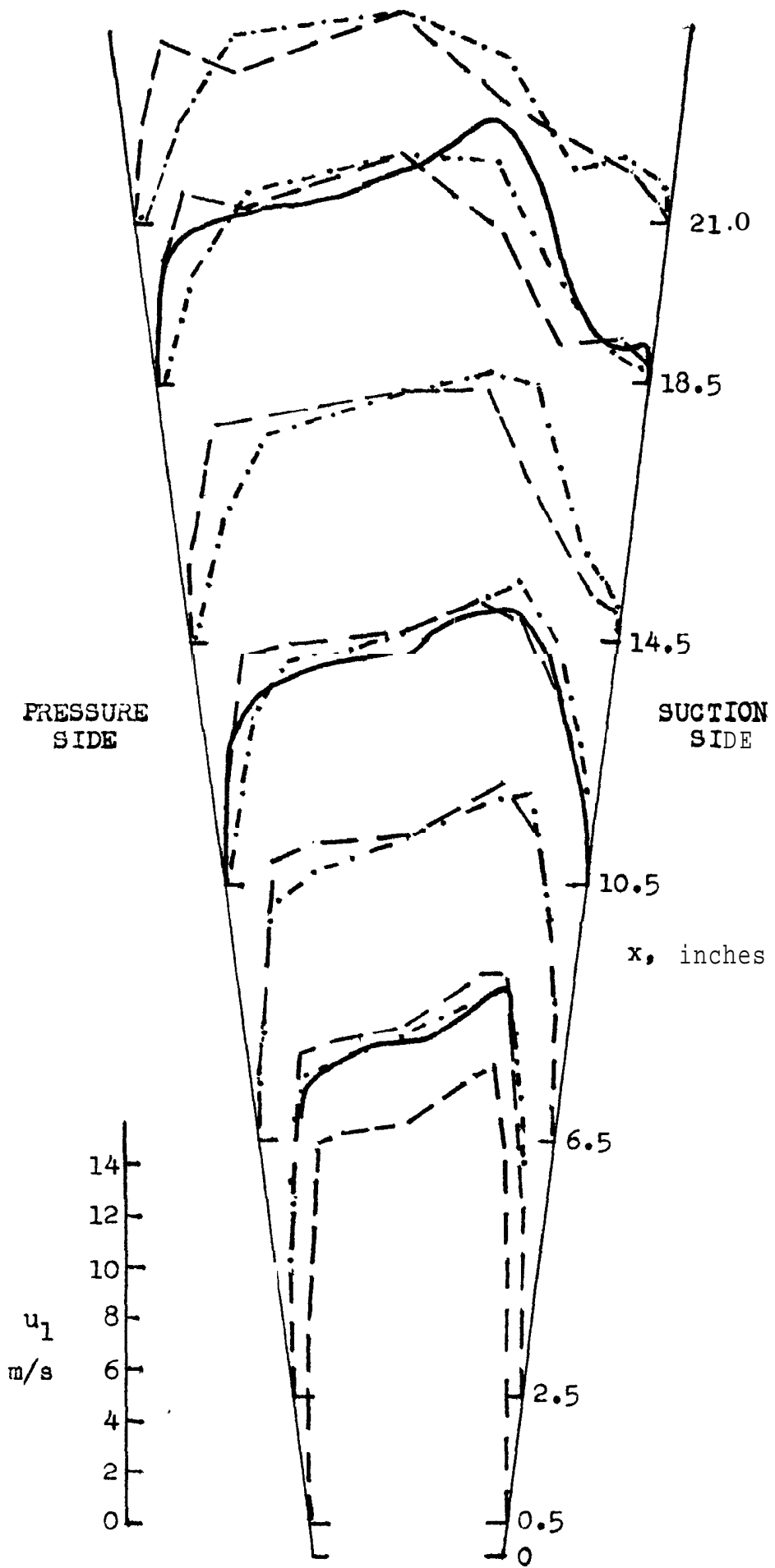


Figure 7. Comparison of calculated and measured radial velocity profiles at channel mid-height.
 _____ measured, - · - · - · - · - · - calculated symmetric flow, -- - - - - calculated asymmetric flow.

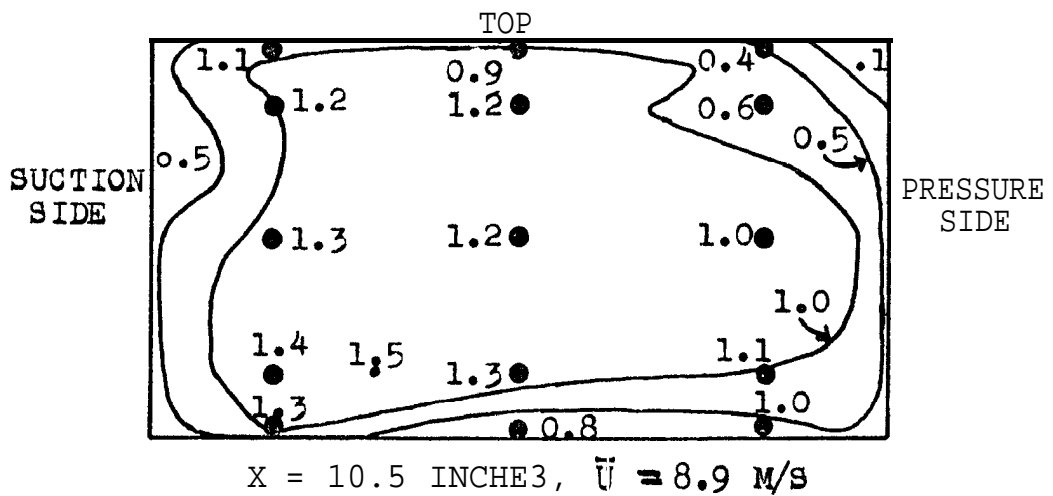
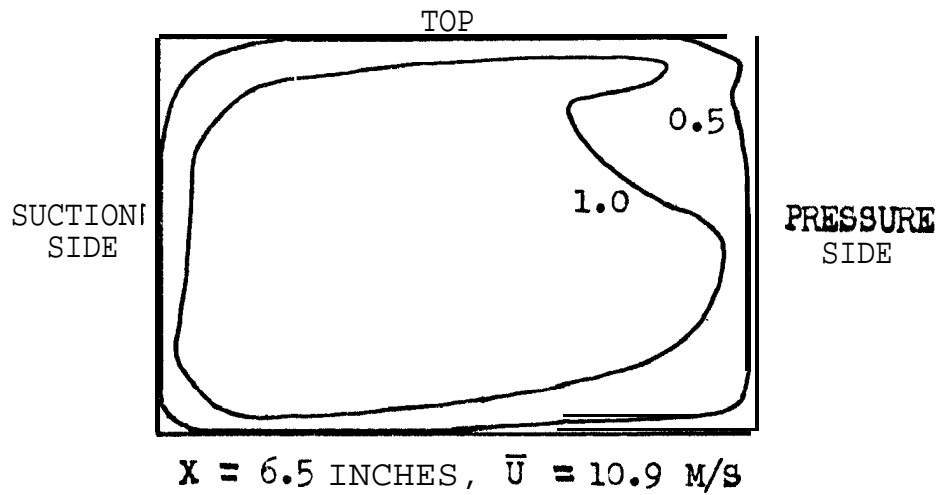
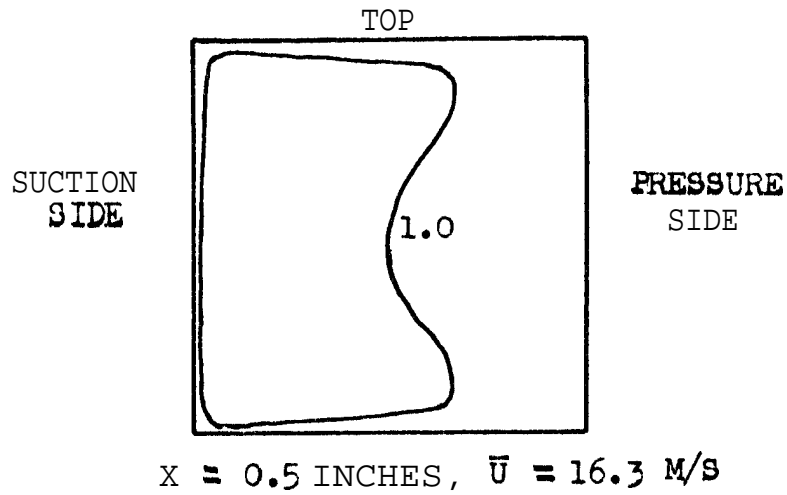


Figure 8. Contours of calculated radial velocity, expressed as a fraction of the local mean velocity, for **asymmetric flow** at $x = 0.5$ and 6.5 inches and at 10.5 inches compared with measured radial velocities at 11 inches. • measured velocities u_1/\bar{u} .

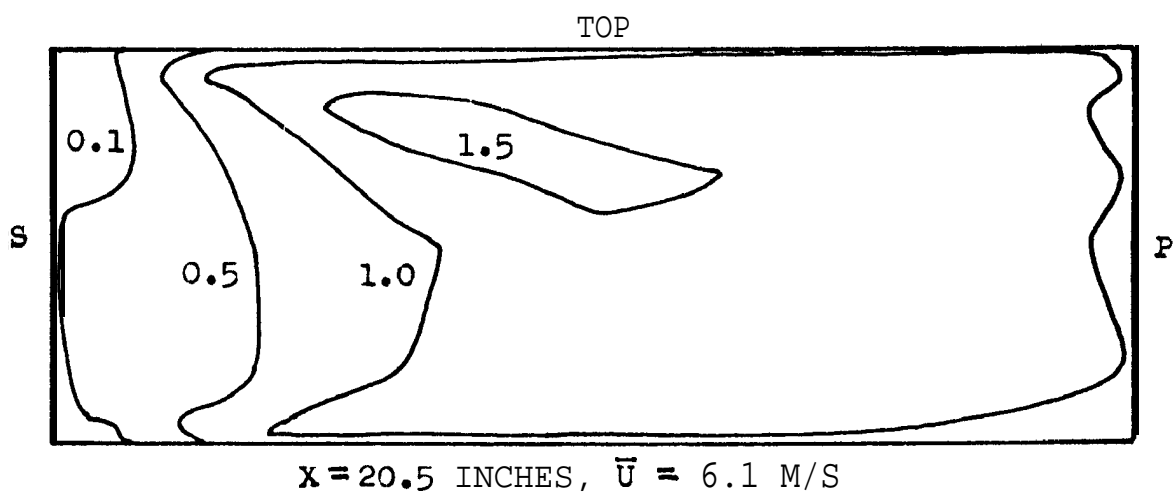
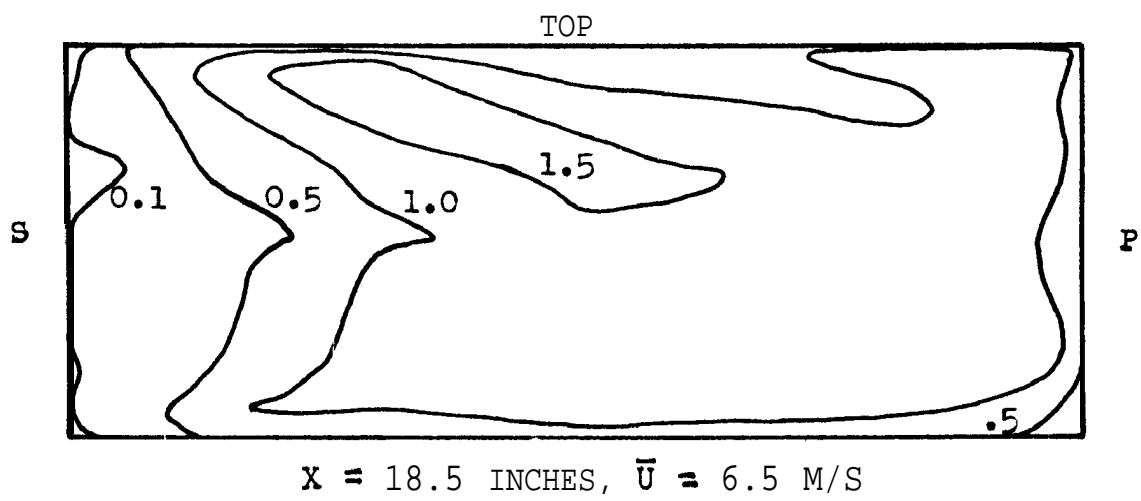
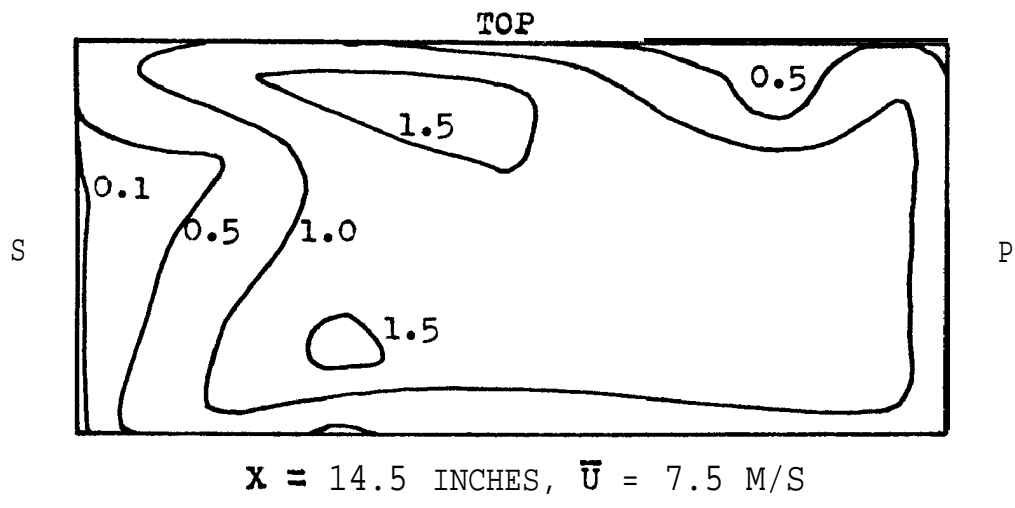


Figure 9. Contours of calculated radial velocity, expressed as a fraction of the local mean velocity, for **asymmetric** flow at $x = 14.5, 18.5$ and 20.5 inches.

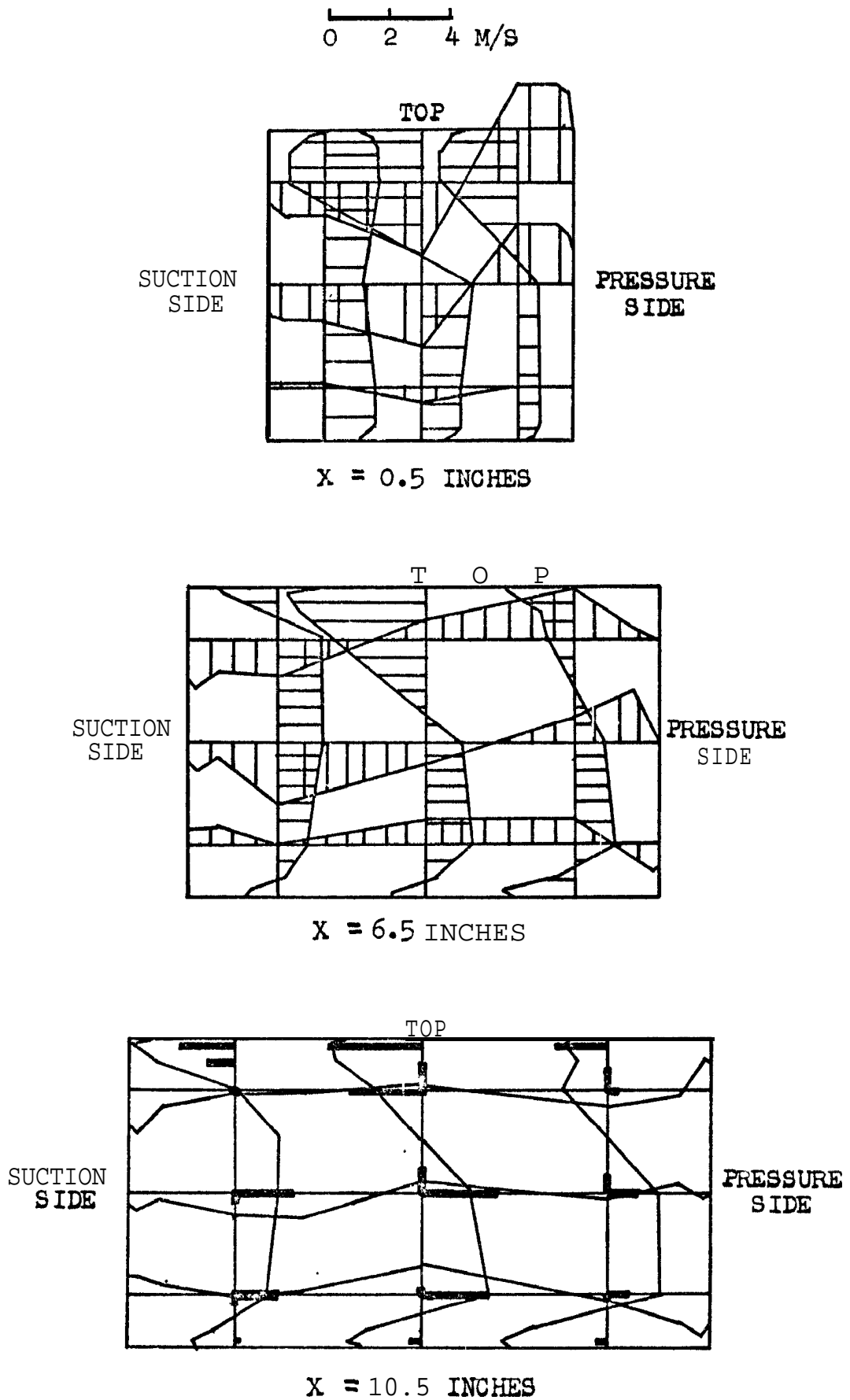
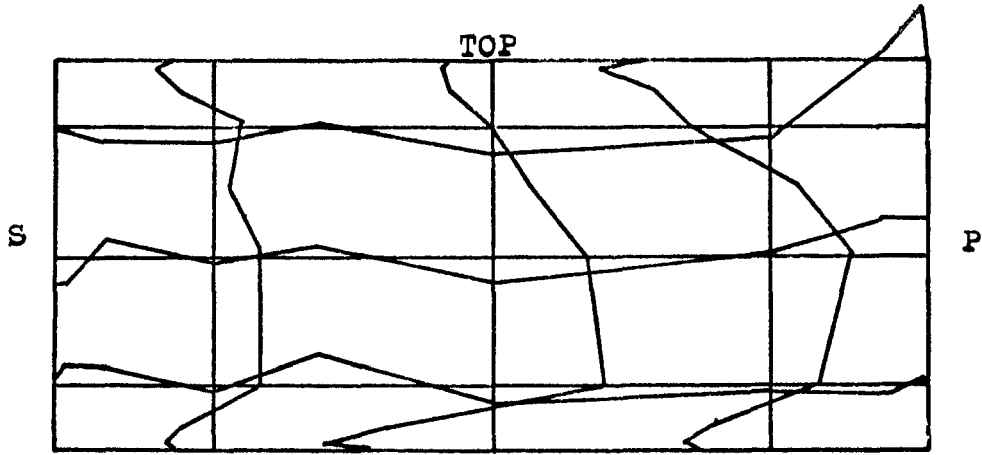
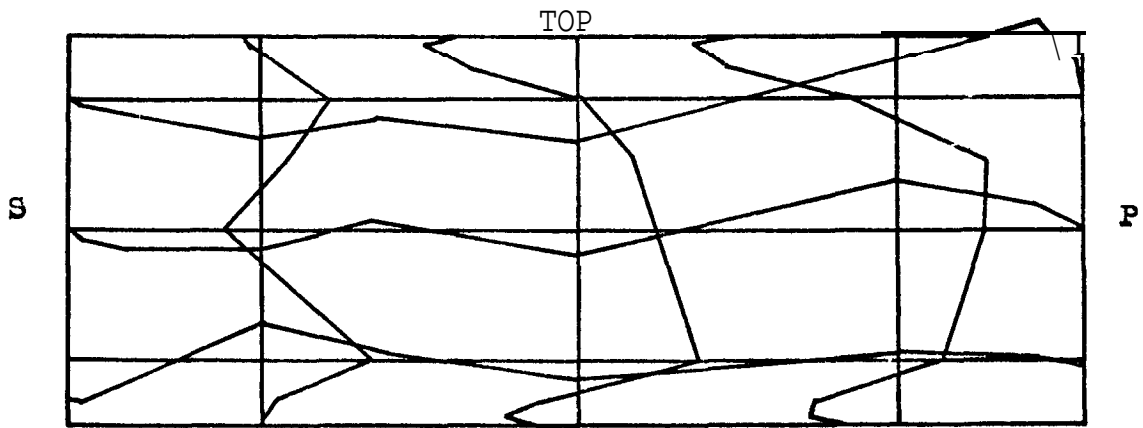


Figure 10. Calculated secondary velocity distributions for asymmetric flow at $x = 0.5$ and 6.5 inches and at $x = 10.5$ Inches compared with measured secondary velocities at 11 Inches. **█** measured.

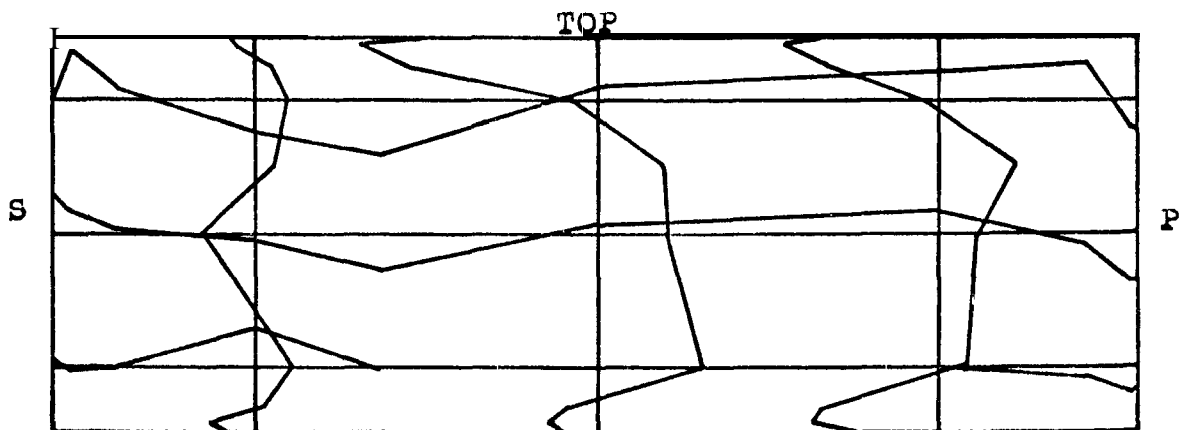
0 2 4 M/S



X = 14.5 INCHES



X = 18.5 INCHES



X = 20.5 INCHES

Figure 11. Calculated secondary velocity distributions for asymmetric flow at $x = 14.5, 18.5$ and 20.5 Inches.

ARC CP No.1384

February 1977

Xoore, J., Moore, J.G. and Johnson, H.W.

ON THREE-DIMENSIONAL FLOW IN CENTRIFUGAL IMPELLERS

Evidence of non-uniform flow at the exit of centrifugal impeller passages is discussed and a Rossby number $W/\omega R_n$ which governs the stable location of wake flow in the exit plane of an impeller is presented. In impellers with large Rossby numbers the stable location of the wake is on the shroud wall; wakes on the suction side wall are stable in impellers with low Rossby numbers,

The/

ARC CP No.1384

February 1977

Xoore, J., Xoore, J.G. and Johnson, M.W.

ON THREE-DIMENSIONAL FLOW IN CENTRIFUGAL IMPELLERS

Evidence of non-uniform flow at the exit of centrifugal impeller passages is discussed and a Rossby number $W/\omega R_n$ which governs the stable location of wake flow in the exit plane of an impeller is presented. In impellers with large Rossby number the stable location of the wake is on the shroud wall; wakes on the suction side wall are stable in impellers with low Rossby numbers.

The/

ARC CP No.1384

February 1977

Xoore, J., Moore, J.G. and Johnson, M.W.

ON THREE-DIMENSIONAL FLOW IN CENTRIFUGAL IMPELLERS

Evidence of non-uniform flow at the exit of centrifugal impeller passages is discussed and a Rossby number $W/\omega R_n$ which governs the stable location of wake flow in the exit plane of an impeller is presented. In impellers with large Rossby numbers the stable location of the wake is on the shroud wall; wakes on the suction side wall are stable in impellers with low Rossby numbers.

The/

ARC CP No.1384

February 1977

Moore, J., Xoore, J.G. and Johnson, M.W.

ON THREE-DIMENSIONAL FLOW IN CENTRIFUGAL IMPELLERS

Evidence of non-uniform flow at the exit of centrifugal impeller passages is discussed and a Rossby number $W/\omega R_n$ which governs the stable location of wake flow in the exit plane of an impeller is presented. In impellers with large Rossby numbers the stable location of the wake is on the shroud wall; wakes on the suction side wall are stable in impellers with low Rossby numbers.

The/

DETACHABLE ABSTRACT CARDS

The ability of a marching-integration procedure to compute a three-dimensional rotating flow with large secondary velocities leading to the formation of a wake is demonstrated. A possible approach to the calculation of three-dimensional impeller flow is suggested.

The ability of a aarching-integration procedure to compute a three-dimensional rotating flow with large secondary velocities leading to the formation of a wake is demonstrated. A possible approach to the calculation of three-dimensional impeller flow is suggested.

The ability of a marching-integration procedure to compute a three-dimensional rotating flow with large secondary velocities leading to the formation of a wake is demonstrated. A possible approach to the calculation of three-dimensional impeller flow is suggested.

The ability of a **marching-integration** procedure to compute a three-dimensional rotating flow with large secondary velocities leading to the formation of a wake is demonstrated. **A possible approach** to the calculation of three-dimensional impeller flow is **suggested**.

©Crown copyright 1977

HER MAJESTY'S STATIONERY OFFICE

Government Bookshops

49 High Holborn, London **WC1V 6HB**

13a Castle Street, Edinburgh **EH2 3AR**

41 The Hayes, Cardiff **CF1 1 JW**

Brazenose Street, Manchester **M60 8AS**

Southey House, **Wine** Street, Bristol **BS1 2BQ**

258 Broad Street, **Birmingham B1 2HE**

80 Chichester Street, Belfast **BT1 4JY**

**Government publications are also available
through booksellers**